Vesicle sizing

Number distributions by dynamic light scattering

F. R. Hallett,* J. Watton,* and P. Krygsman‡

*Guelph-Waterloo Program for Graduate Work in Physics, Department of Physics, University of Guelph, Guelph, Ontario N1G 2W1; and ‡Guelph-Waterloo Centre for Graduate Work in Chemistry, Department of Chemistry, University of Guelph, Guelph, Ontario N1G 2W1 Canada

ABSTRACT A procedure is described which optimizes nonnegative least squares and exponential sampling fitting methods for analysis of dynamic light scattering (DLS) data from aqueous suspensions of vesicle/liposome systems. This approach utilizes a Rayleigh-Gans-Debye form factor for a coated sphere and yields number distributions which can be compared directly to distributions obtained by freeze-fracture electron microscopy (EM). Excellent agreement between the DLS and EM results are obtained for vesicle size distributions in the 100–200-nm range.

INTRODUCTION

Dynamic light scattering (DLS) has been regularly used to obtain size information from aqueous suspensions of vesicles or liposomes (1–20). The majority of these investigations used the method of cumulants, sometimes termed moments analysis, to analyze the experimental light scattering data. In its simplest form, the method of cumulants provides information on the mean size of the sample and on the width of the size distribution (21). This information is, however, in the form of intensity-averaged quantities which correspond to the statistical properties of a distribution which describes the amount of light scattered by each particle size. Thus, the intensity-average radius, $\overline{R}_I$, is given by (22)

$$\overline{R}_I = \frac{\sum_i N_i M_i^2 P(R_i) R_i}{\sum_i N_i M_i^2 P(R_i)} \tag{1}$$

in which N_i is the fraction of particles having radius R_i, mass M_i, and $P(R_i)$ is the single particle scattering factor. The most common assumption is to set $P(R_i) = 1$ for all R_i which implies that the particles are point scatterers. Under this assumption, the resulting parameters are called z-average quantities. Thus, the z-average radius is

$$\overline{R}_z = \frac{\sum_i N_i M_i^2 R_i}{\sum_i N_i M_i^2} \tag{2}$$

or, using weight fraction $\omega_i = N_i M_i$, then

$$\overline{R}_z = \frac{\sum_i \omega_i M_i R_i}{\sum_i \omega_i M_i}. \tag{3}$$

Other techniques, such as electron microscopy, yield number average quantities. For example, the number average radius, $\overline{R}_N$, is simply

$$\overline{R}_N = \frac{\sum_i N_i R_i}{\sum_i N_i}. \tag{4}$$

Clearly, R_i can differ significantly from $\overline{R}_z$ if $P(R) \neq 1$ and both $\overline{R}_I$, $\overline{R}_z$ can differ significantly from $\overline{R}_N$, depending on the breadth and shape of the size distribution. The three quantities can be identical only in the case of an infinitely narrow size distribution of point scatterers.

Several attempts have been made to extract number average information by cumulants analysis of DLS data from vesicles. Selser and Yeh (23) assumed that $P(R) = 1$ for all vesicles in the sample and that the skewness and higher moments of the size distribution were negligible. They obtained the expression

$$\overline{R}_N = \frac{A}{D_z(1 + 3\delta_z)}, \tag{5}$$

where D_z is the z-average diffusion coefficient which can be related to $\overline{R}_z$ by the Stokes-Einstein equation

$$\overline{R}_z = \frac{A}{D_z} \tag{6}$$

and δ_z is the relative dispersion of D_z,

$$\delta_z = \frac{\langle D^2 \rangle_z}{\langle D_z \rangle^2} - 1. \tag{7}$$

Both D_z and δ_z can be obtained from the first and second cumulants, respectively.

Goll and Stock (6) and Goll et al. (7) described an elegant method in which size distributions were approxi-

0006-3495/91/02/357/06 $2.00

mated by piece-wise linear functions called first order splines. Their approach also incorporated a Rayleigh-Gans-Debye (RGD) form factor for a coated sphere that allowed an improved estimate of $P(R)$ to be included in the analysis. In principle, this approach was a good one; good fits to the experimental light scattering data were obtained and mass density distributions of the vesicle suspensions were determined. In practice, the method of splines has not been broadly used partly because it involves a priori knowledge of the optimum number of splines and spline-boundaries or "knots" and partly because other discrete inversion methods such as the Provencher method (24) and exponential sampling (25) have gained wider acceptance.

McCracken and Sammons (17) have used the Provencher method in a comparative study involving DLS, electron microscopy, and ultracentrifugation. However, they assumed that $P(R) = 1$ for all samples studied. This assumption was also made by Miyamoto et al. (19) in a study of brush border membrane vesicles. They interpreted the nonscaling of the vesicle sizes with scattering vector to be indicative of ellipticity of the vesicles and subsequently developed a theory (26) of scattering from thinly coated ellipsoids. The nonscaling which they observed however, may be due to the lack of an appropriate scattering factor $P(R)$ in the original analysis.

As has just been described, a substantial number of analytic methods have been employed to analyze DLS data from vesicle systems. Only recently (27) has there been an attempt to employ modern fitting techniques along with the appropriate RGD or Mie form factor for a vesicle system. However, this study was limited to very small vesicle systems for which the incorporation of a form factor was of marginal benefit. We will now describe an improved approach which incorporates an RGD form factor into an exponential sampling analysis which has been modified to include a nonnegative least squares fitting procedure. This method is suitable for study of vesicle distributions in the ≤ 300-nm size range. A similar Mie analysis is being developed for study of even larger vesicle/liposome systems.

THEORY

The nonnegative least squares (NNLS) modification of exponential sampling was first described by Morrison et al. (28). The objective was to minimize

$$\text{var} = [g^{(1)}(\tau) - \sum_{n=1}^{N} a_n M^2 P(R) \exp(-\Gamma_n \tau)]^2 \quad (8)$$

with respect to the a_n's, which correspond to the relative abundances of each size in the distribution. In this equation, $g^{(1)}(\tau)$ represents the electric field autocorrelation function which is obtained from DLS experiments,

$$g^{(1)}(\tau) = \int G(\Gamma) \exp(-\Gamma\tau)\, d\Gamma, \quad (9)$$

where $\Gamma = DQ^2$ is a decay coefficient, D is the diffusion coefficient, and Q is the scattering vector. Thus the a_n's in Eq. 8 are a discrete representation or histogram of the distribution of decay rates $G(\Gamma)$ arising from the size distribution of the scatterers. Conversion to $G(R)$, the size distribution, is easily achieved using the relation

$$G(R)dR = G(\Gamma)d\Gamma. \quad (10)$$

In practice, direct inclusion of $P(R)$ in Eq. 8 can lead to spurious oscillations in $G(R)$. This is because the $P(R)$ can be calculated at the precise value of R corresponding to Γ_n whereas each of the Γ_n's have an associated width or resolution. To avoid these problems, Hallett et al. (29) used triangles instead of delta functions in Γ space and averaged the scattering factors over these triangles. While such a method involves numerical integration and is computationally more intensive, it does yield smooth accurate size distributions. In this formalism, Eq. 8 becomes

$$\text{var} = [g^{(1)}(\tau) - \sum_{n=1}^{N} a_n \int V_c^2 P(R) C_n(\tau)\, d\Gamma]^2 \quad (11)$$

in which $C_n(\tau)$ corresponds to the triangles,

$$C_n(\tau) = \frac{1}{\tau^2(\alpha - 1)\Gamma_n}[\alpha e^{-\Gamma_{n-1}\tau} - (1 + \alpha)e^{-\Gamma_n\tau} + e^{-\alpha\Gamma_{n+1}\tau}], \quad (12)$$

where $\alpha = \exp(\pi/\omega_{max})$ defines the resolution or base of the triangle and in which V_c is the coat volume. $P(R)$ now corresponds to the single particle scattering factor for a coated sphere of radius R.

Several choices are available for determining the form factor, $F(R)$, from which, for optically isotropic, spherical scatterers, $P(R)$ can be obtained $[P(R) = [F(R)]^2]$.

The simplest RGD formulation for $F(R)$ arises from the assumption (see Fig. 1) that refractive indices of the lumen, n_2, and medium, n_0, are identical and has the form (30)

$$F(R) = [3/x^3(1 - \gamma^3)] \cdot [\sin x - \sin \gamma x - x \cos x + \gamma x \cos \gamma x], \quad (13)$$

where $\gamma = R_{int}/R$ and $x = RQ$. R_{int} is the interior radius of the vesicle and Q is the scattering vector. For thinly

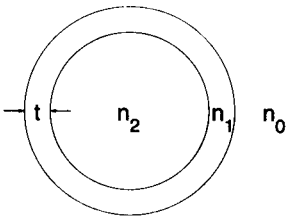

FIGURE 1 Optical model of a vesicle; n_0, n_1, and n_2 are refractive indices of the medium, coat, and lumen, respectively, and t is the coat thickness.

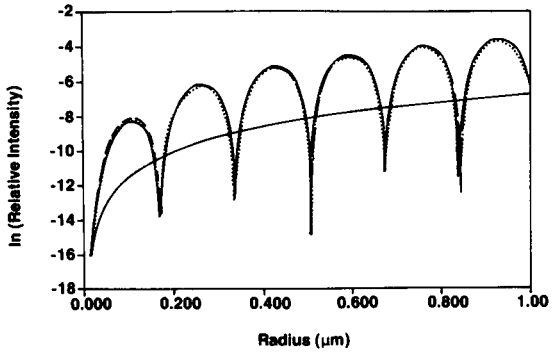

FIGURE 2 Relative scattering intensities for a vesicle system with n_0, n_1, and n_2 equalling 1.33, 1.42, 1.33, respectively, and calculated as a function of vesicle radius. Various curves are coat volume squared (*solid line*), Mie calculation (*solid line*), Eq. 13 (*long dashes*), Eq. 14 (*short dashes*), Eq. 16 (*dots*). The scattering angle was 90° and laser wavelength was 632.8 nm for all cases.

coated spheres $\gamma \approx 1$ and Eq. 13 reduces to

$$F(R) = \frac{\sin x}{x}. \tag{14}$$

The total scattered intensity per particle with coat volume $V_c = 4\pi t(R - t/2)^2$ is

$$I_p(R) \propto V_c^2[F(R)]^2 = V_c^2 P(R). \tag{15}$$

A more general RGD approach to calculating $I_p(R)$ has been described by Wyatt (31). This formulation includes the relative refractive indices of the coat, $m_1 = n_1/n_0$, and the lumen, $m_2 = n_2/n_0$, to obtain

$$I_p(R) = \left[\frac{(m_1 - 1)}{2\pi}\frac{(4\pi R^3)}{3}\left[\frac{3j_1(x)}{x} + f^3\frac{(m_2 - m_1)}{(m_1 - 1)}\frac{3j_1(fx)}{fx}\right]\right]^2. \tag{16}$$

In this expression, $j_1(x)$ is the first order spherical Bessel function and

$$f = 1 - \frac{t}{R}. \tag{17}$$

Finally, we have recently, in our own laboratory, developed a program which uses a complete Mie calculation to determine $I_p(R)$ for vesicles. Fig. 2 shows a comparison of relative scattering intensities as a function of R for vesicle systems having $n_2 = n_0 = 1.33$ and with a membrane thickness of 0.01 μm. The refractive index of the coat was chosen to be 1.42 for comparison purposes only. Because the curves superimpose, the figure shows definitively that unilamellar vesicles, whose membranes are generally <0.01 μm in thickness are well represented by the thin coat approximation and that Eq. 14 is a perfectly good approximation for particles up to a micron or more in diameter. However, this approximation holds only if the refractive index of the lumen and the medium are identical. Preliminary Mie computations have indicated that differences between n_2 and n_0 as small as 0.01 cannot only cause Eq. 14 to break down, but the whole RGD approximation as well. This sensitivity is presumably due to the vesicle assuming some of the scattering characteristics of a uniform sphere as opposed to those of a shell. These studies will be described more fully in a subsequent publication.

Because the vesicles in this study were prepared under conditions in which $n_2 = n_0$, we have used either Eq. 13 or Eq. 14 in all analyses.

ELECTRON MICROSCOPY

The recovery of vesicle size distributions from freeze-fracture electron micrographs is not a simple procedure. Recently, we have provided a method whereby the vesicle size distribution may be estimated from the distribution of image sizes measured on the electron micrographs (32). This method is based on the assumption that vesicles are randomly cleaved by the fracture plane. We were able to show that the average image radius $\bar{r}$ and the average vesicle radius $\bar{R}$ are simply related by

$$\bar{R} = \frac{4}{\pi}\bar{r}. \tag{18}$$

By inputting a relatively simple parameterized function, $G(R)$, for the distribution of vesicle radii,

$$G(R) = \frac{1}{m!}\left(\frac{m+1}{\bar{R}}\right)^{m+1} R^m \exp\left(-\frac{R(m+1)}{\bar{R}}\right) \tag{19}$$

in the expression for $Y(r)$, the distribution of image radii, which is

$$Y(r) = \int_r^\infty \frac{r}{R(R^2 - r^2)^{1/2}} G(R)\, dR \qquad (20)$$

one obtains

$$Y(r) = \frac{1}{2^{m-2}m!}\frac{\beta^{m+1}}{r}\left\{K_{m-1}(\beta) + \frac{(m-1)!}{(m-2)!}K_{m-3}(\beta) + \cdots \right.$$
$$\left. \frac{(m-1)!}{\frac{(m-1)!}{2}\left[m - \frac{m}{2} - \frac{1}{2}\right]!} K_0\beta \right\} \qquad (21)$$

where

$$\beta = \frac{\pi(m+1)r}{4\bar{r}}. \qquad (22)$$

This function requires as input parameters, both $\bar{r}$, the average image radius, and m, which is an integer. The factor m is adjusted until one obtains the best agreement between Eq. 21 and the experimental image distribution. Once m which yields the best fit is obtained, then m and $\bar{R}$ (from Eq. 18) can be used to estimate the vesicle size distribution $G(R)$ for comparison to the DLS results.

EXPERIMENTAL METHODS

Unilamellar vesicles of dimyristoylphosphatidylcholine (DMPC) (Sigma Chemical Company, St. Louis, MO) were prepared by extrusion using a method similar to that of Hope et al. (33) and Olson et al. (34). The dry, pure DMPC was vortexed in 0.05 M phosphate buffer (pH 7.4) and then extruded at least 10 times through two stacked polycarbonate filters (100 or 200 nm pore size, from Nucleopore Corp., Pleasanton, CA) using pressures of up to 5.6×10^5 Pa from a nitrogen gas cylinder. Samples were divided into separate aliquots for freeze fracture electron microscopy and for DLS measurements. Details on the freeze fracture procedures are published elsewhere (32). In the case of light scattering, the original aliquots, which were typically 55–145 mM DMPC were diluted 1:100 using the original buffer. This insured that samples were dilute enough for DLS experiments and also that the lumen and medium were identical in concentration and, more importantly, refractive index.

The DLS apparatus used in these studies has been described in a previous publication (29) and all data analysis was performed on a microcomputer using the FORTRAN programming language. The numerical integrations in Eq. 11 were performed using Simpson's rule with 60 divisions per triangle. The program to calculate Mie coefficients for vesicles was written by ourselves, but based, in part, on a similar program of Bohren and Huffman (35).

RESULTS AND DISCUSSION

The objective of this study was to provide a comparison between the DLS results, obtained using the analysis procedures described in earlier sections, and the results, on the same sample, from a completely independent technique, freeze fracture electron microscopy (FFEM). The amount of effort involved in hand measuring the size of thousands of FFEM images was significant so that we had to be very selective of the samples chosen in order for the comparison to be as rigorous and general as possible. For these reasons, we examined two preparations of vesicles which will be called Sample 1 and Sample 2. The DLS results indicated that Sample 1 contained a narrow unimodal distribution and Sample 2 contained bimodal and broader distributions.

The distribution of image radii obtained from electron

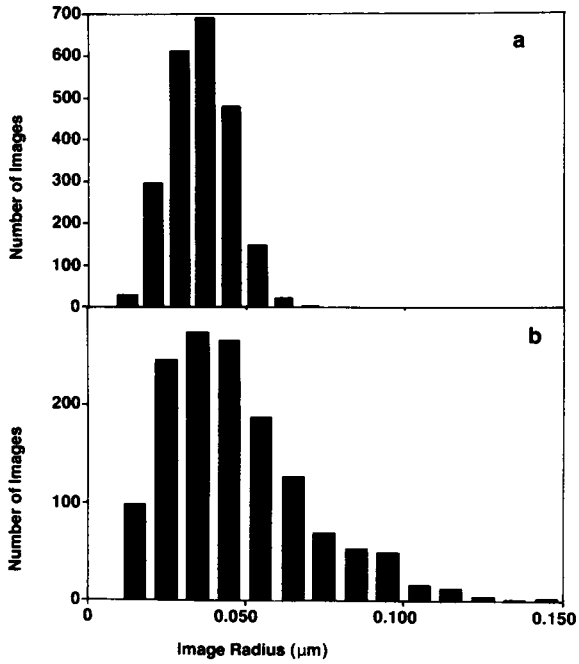

FIGURE 3 The distribution of image radii as determined from the analysis of electron micrographs of Sample 1 (*a*) and Sample 2 (*b*).

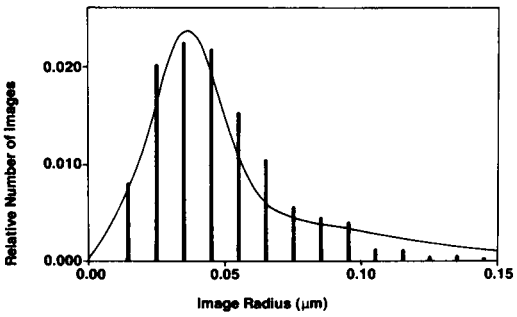

FIGURE 4 The distribution of freeze fracture image radii for Sample 2 (*histogram*) and a trial and error estimate of the best fit of two image distributions computed using Eq. 21 (*smooth line*).

TABLE 1

Sample	Filter radius	DLS average radius no form factor	DLS average radius with form factor	EM average radius
	μm	μm	μm	μm
1	0.05	0.052	0.045	0.045
2	0.10	0.096	0.063	0.060

micrographs for Sample 1 and Sample 2 are shown in Fig. 3. Even though the process of freeze fracturing tends to smear the bimodality of Sample 2 (because the fracture plane tends to randomly cleave the vesicles), the distribution of image sizes does hint at the likelihood of two overlapping distributions. A fit of Eq. 21 to the image distributions for Sample 1 was simple in that $\bar{r}$ was obtained from the measurements and m was determined simply by stepping through the integer values until best agreement was obtained. However, the optimum values of m and $\bar{r}$ for each of the two distributions (a and b) in Sample 2 were much more difficult to find. A least squares fitting routine to accomplish the task would involve five parameters ($\bar{r}_a$, m_a, $\bar{r}_b$, m_b, and α) where α and $(1 - \alpha)$ would describe the relative fraction of the sample belonging to distributions a and b, respectively. Such a five-parameter fit to 15 data points was judged to be questionable, however, with results being almost as uncertain as fits based on trial and error estimates of the five parameters. As a result, trial and error methods were used to obtain the "best fit" to Sample 2 (Fig. 4). We do not claim that this fit is the best possible nor do we suggest that we have uniquely determined the five parameters. We do claim, however, that a bimodal distribution similar to that shown is better than a unimodal distribution at fitting the Sample 2 data. Table 1 lists the average vesicle sizes obtained from these image size measurements.

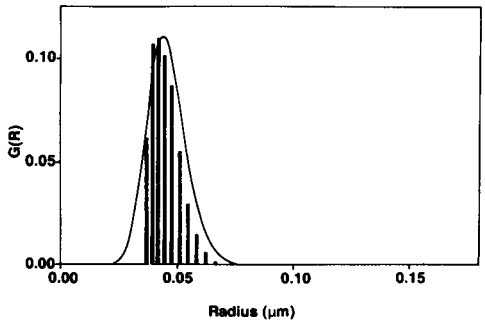

FIGURE 5 A comparison of DLS and EM results obtained from Sample 1.

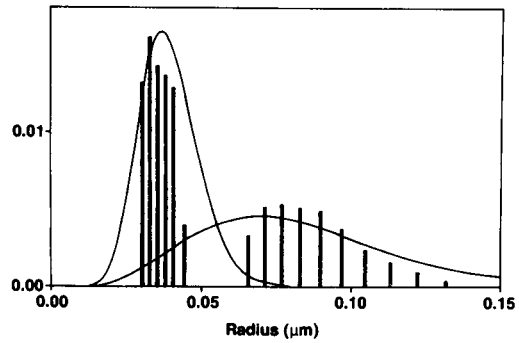

FIGURE 6 A comparison of DLS and EM results obtained from Sample 2.

Once $\bar{r}$ and m are known for any image distribution, it is straightforward to estimate the distribution of vesicle radii using Eqs. 18 and 19. These estimated distributions are provided in Figs. 5 and 6and correspond to the solid line curves in each case. In Fig. 5, we compare the light scattering results (histogram) to the electron microscopic results (smooth line) for Sample 1. Fig. 6 provides a similar comparison for Sample 2. The importance of including the form factor in the analysis is clearly demonstrated in Table 1. The difference between intensity average and number average radius is significant for both samples studied. In the case of Sample 1, the inclusion of the vesicle form factor lowers the value of the average radius by $\sim 14\%$ and brings it into line with the results from electron microscopy. The effect is even more striking for larger vesicles as in Sample 2, where the difference between the intensity average and the number average radius is $\sim 30\%$. The difference is expected to be even larger as the vesicle size increases.

CONCLUSION

The inclusion of a vesicle form factor, in the triangle method of exponential sampling, leads to vesicle size distributions which compare extremely well to those obtained by freeze fracture electron microscopy. This applies for spherical unilamellar vesicles with diameters < 0.3 μm. We are now investigating the application of DLS with Mie form factors to the sizing of larger vesicle systems.

We gratefully acknowledge the technical assistance of J. Marsh and David Morris in the acquisition of the DLS and EM data.

This project was supported by a grant from the Natural Science and Engineering Research Council of Canada.

REFERENCES

1. Selser, J. C., Y. Yeh, and R. J. Baskin. 1976. A light-scattering characterization of membrane vesicles. *Biophys. J.* 16:337–356.
2. Selser, J. C., Y. Yeh, and R. J. Baskin. 1976. A light-scattering measurement of membrane vesicle permeability. *Biophys. J.* 16:1557–1371.
3. Chen, F. C., A. Chrzeszczyk, and B. Chu. 1977. Quasielastic laser light scattering of monolayer vesicles. *J. Chem. Phys.* 66:2237–2238.
4. Day, E. P., J. T. Ho, R. K. Kunze Jr., and S. T. Sun. 1977. Dynamic light scattering study of calcium-induced fusion in phospholipid vesicles. *Biochim. Biophys. Acta.* 470:503–508.
5. Ostrowsky, N., and Ch. Hesse-Bezot. 1977. Dynamic light scattering study of the conformational change and fusion phenomenon of phospholipid vesicles . *Chem. Phys. Lett.* 52:141–144.
6. Goll, J. H., and G. B. Stock. 1977. Determination by photon correlation spectroscopy of particle size distributions in lipid vesicle suspensions. *Biophys. J.* 19:265–273.
7. Goll, J., F. D. Carlson, Y. Barenholz, B. J. Litman, and T. E. Thompson. 1982. Photon correlation spectroscopic study of the size distribution of phospholipid vesicles. *Biophys. J.* 38:7–13.
8. Kippenberger, D., K. Rosenquist, L. Odberg, P. Tundo, and J. H. Fendler. 1983. Polymeric surfactant vesicles. Synthesis and characterization by nuclear magnetic resonance spectroscopy and dynamic laser light scattering. *J. Am. Chem. Soc.* 105:1129–1135.
9. Muddle, A. G., and J. S. Higgins. 1983. Light scattering and neutron scattering from concentrated dispersions of small unilamellar vesicles. *Faraday Discuss. Chem. Soc.* 76:77–92.
10. Schurtenberger, P., and H. Hauser. 1984. Characterization of the size distribution of unilamellar vesicles by gel filtration, quasi-elastic light scattering and electron microscopy. *Biochim. Biophys. Acta.* 778:470–480.
11. Perevucnik, G., P. Schurtenberger, D. D. Lasic, and H. Hauser. 1985. Size analysis of biological membrane vesicles by gel filtration, dynamic light scattering and electron microscopy. *Biochim. Biophys. Acta.* 821:169–173.
12. Hantz, E., A. Cao, J. Escaig, and E. Taillandier. 1986. The osmotic response of large unilamellar vesicles studied by quasielastic light scattering. *Biochim. Biophys. Acta.* 862:379–386.
13. Li, W., T. S. Aurora, T. H. Haines, and H. Z. Cummins. 1986. Elasticity of synthetic phospholipid vesicles and submitochondrial particles during osmotic swelling. *Biochemistry.* 25:8220–8229.
14. Li, W., and T. H. Haines. 1986. Uniform preparations of large unilamellar vesicles containing anionic lipids. *Biochemistry.* 25: 7477–7483.
15. Mayler, L. D., M. J. Hope, and P. R. Cullis. 1986. Vesicles of variable sizes produced by a rapid extrusion procedure. *Biochim. Biophys. Acta.* 858:161–168.
16. Haines, T. H., W. Li, M. Green, and H. Z. Cummins. 1987. The elasticity of uniform, unilamellar vesicles of acidic phospholipids during osmotic swelling is dominated by the ionic strength of the media. *Biochemistry.* 26:5439–5447.
17. McCracken, M. S., and M. C. Sammons. 1987. Sizing of a vesicle drug formulation by quasi-elastic light scattering and comparison with electron microscopy and ultracentrifugation. *J. Pharm. Sci.* 76:56–59.
18. Sattelle, D. B., K. H. Langley, A. L. Obaid, and B. M. Salzberg. 1987. Laser light scattering determination of size and dispersity of synaptosomes and synaptic vesicles isolated from squid (Loligo pealei) optic lobes. *Eur. Biophys. J.* 15:71–76.
19. Miyamoto, S., T. Maeda, and S. Fujime. 1988. Change in membrane elastic modulus on activation of glucose transport system of brush border membrane vesicles studied by osmotic swelling and dynamic light scattering. *Biophys. J.* 53:505–512.
20. Rivière, M-E., G. Johannin, D. Gamet, V. Molitor, G. A. Peschek, and B. Arrio. 1988. Laser light scattering techniques for determining size and surface charges of membrane vesicles from cyanobacteria. *Methods Enzymol.* 167:691–700.
21. Koppel, D. E. 1972. Analysis of macromolecular polydispersity in intensity correlation spectroscopy: the method of cumulants. *J. Chem. Phys.* 57:4814–4820.
22. Burchard, W. 1979. Quasi-elastic light scattering: separability of effects of polydispersity and internal modes of motion. *Polymer.* 20:577–581.
23. Selser, J. C., and Y. Yeh. 1976. A light scattering method of measuring membrane vesicle number-averaged size and size dispersion. *Biophys. J.* 16:847–848.
24. Provencher, S. W. 1982. CONTIN: a general purpose constrained regularization program for inverting noisy linear algebraic and integral equations. *Comp. Phys. Comm.* 27:229–242.
25. Pike, E. R., D. Watson, and F. M. Watson. 1983. Analysis of polydisperse scattering data II. *In* Measurement of Suspended Particles by Quasi-elastic Light Scattering. B. E. Dahneke, editor. 107–128.
26. Fujime, S., M. Takasaki-Ohsita, and S. Miyamoto. 1988. Dynamic light scattering from polydisperse suspensions of thin ellipsoidal shells of revolution with submicron diameters. *Biophys. J.* 53:497–503.
27. Ruf, H., Y. Georgalis, and E. Grell. 1989. Dynamic laser light scattering to determine size distributions of vesicles. *Methods Enzymol.* 172:364–390.
28. Morrison, I. D., E. F. Grabowski, and C. A. Herb. 1985. Improved techniques for particle size determination by quasi-electric light scattering. *Langmuir.* 1:496–501.
29. Hallett, F. R., T. Craig, J. Marsh, and B. Nickel. 1989. Particle size analysis: number distributions by dynamic light scattering. *Can. J. Spectrosc.* 34:63–70.
30. Aragón, S. R., and R. Pecora. 1982. Anisotropic light scattering from phospholipid vesicles. *J. Colloid. Interface Sci.* 89:170–184.
31. Wyatt, P. J. 1973. Differential light scattering techniques for microbiology. *In* Methods in Microbiology. J. R. Norris and D. W. Ribbons, editors. Academic Press, New York. 8:183–263.
32. Hallett, F. R., B. Nickel, C. Samuels, and P. Krygsman. Determination of vesicle size distributions by freeze-fracture electron microscopy. *J. El. Microscopy Techniques.* In press.
33. Hope, M. J., M. B. Bally, G. Webb, and P. R. Cullis. 1985. Production of large unilamellar vesicles by a rapid extrusion procedure. Characterization of size distribution, trapped volume and ability to maintain a membrane potential. *Biochim. Biophys. Acta.* 812:55–65.
34. Olson, F., C. A. Hunt, F. C. Szoka, W. J. Vail, and D. Papahadjopoulos. 1979. Preparation of liposomes of defined size distribution by extrusion through polycarbonate membranes. *Biochim. Biophys. Acta.* 557:9–23.
35. Bohren, C. F., and D. R. Huffman. 1983. Absorption and Scattering of Light by Small Particles. John Wiley and Sons, New York. 483–489.